# STUDY OF THE ELECTRON BEAM DYNAMICS IN THE FERMI @ ELETTRA LINAC

M. Cornacchia, P. Craievich, S. Di Mitri, Sincrotrone Trieste, Trieste, Italy
I. Pogorelov, J. Qiang, M. Venturini, A. Zholents [#], LBNL, Berkeley, CA 94720, U.S.A.
D. Wang, MIT, Cambridge, MA 02139, U.S.A.,
R. Warnock, SLAC, Stanford, CA 94025, U.S.A.

*Abstract*

A study of the electron beam dynamics in the linac is conducted for the FERMI free electron laser (FEL) founded for construction at the Sincrotrone Trieste [1].

## LAYOUT AND DESIGN PARAMETERS

The FERMI accelerator layout is schematically shown in Figure 1. It consists of an injector, four linacs, two bunch compressors, a laser heater, and a spreader used to direct the electron beam into one of two undulator lines.

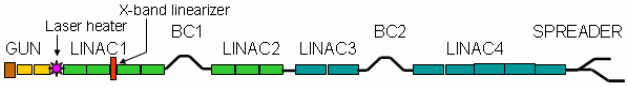


Figure 1 A schematic of the FERMI accelerator. The entire length of the machine ~ 150 m.

The electron beam energy after injector at the entrance of the laser heater is ~100 MeV and the peak current is ~70A. At the exit of Linac 4 the electron beam energy is approximately 1.2 GeV and the electron peak current is 500 A or 800 A, depending on the bunch length needed by the FEL processes. Three options have been developed: the short bunch (SB) option [2] with a bunch length ~ 200 fs, the medium bunch (MB) option with a bunch length ~ 700 fs and the long bunch (LB) option with a bunch length ~ 1.4 ps. The accelerator was designed with sufficient flexibility to accommodate such variations in bunch parameters. Only the medium and long bunch options are considered here. Other important electron beam parameters include the normalized slice electron beam emittance and the slice energy spread, which are 1.5 micron and 150 keV respectively for all three bunch lengths. Table 1 shows a list of major design parameters. A new parameter, the "flatness", defines the value of the quadratic component of energy variation along the bunch for which the increase in bandwidth of the x-ray signal due to this variation becomes equal to the Fourier transform limited bandwidth defined by the bunch length.

Table 1: Main electron beam parameters

| | Medium | Long |
|---|---|---|
| Bunch length, ps (flat part) | 0.7 | 1.4 |
| Peak current, A | 500 | 800 |
| Emittance (slice), μm | <1.5 | <1.5 |
| Energy spread (slice), keV | <150 | <150 |
| Flatness, $\|d^2E/dt^2\|$, MeV/ps$^2$ | <0.8 | <0.2 |

[#]AAZholents@lbl.gov

Table 1 indicates that the operation of the FERMI FEL requires high peak current, low emittance and low energy spread. The injector provides the low emittance and energy spread, while the accelerator must provide the high peak current. Preservation of the beam quality during bunch compression and acceleration is the most challenging task of the accelerator optimization study.

## BEAM QUALITY PRESERVATION

### *Slice Emittance*

Figure 2 shows the accelerator lattice. Small beta-functions were produced in BC1, BC2 and spreader in order to minimize emittance excitation due to coherent

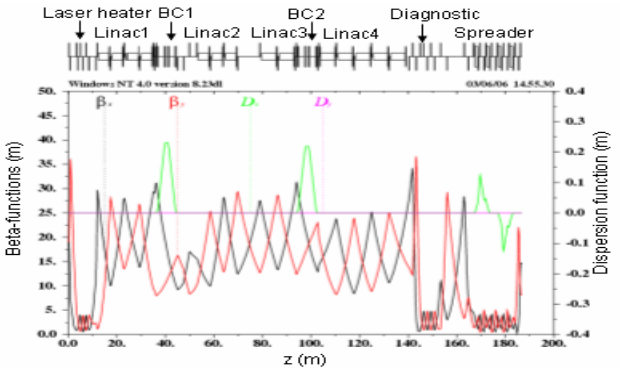


Figure 2 Twiss function of the FERMI accelerator.

synchrotron radiation (CSR). The spreader lattice has been designed in a "dog-leg" configuration with a $-I$ transport between adjacent bends which allows self-cancellation of the emittance excitation due to CSR in the bends. As the result of these precautions, neither the MB nor LB case showed an increase in the slice emittance in simulations performed with *Elegant* [3].

### *Slice Energy Spread*

The slice energy spread is small in the electron beam exiting the injector, but grows further down the linac due to the microbunching instability [4-7] driven by the longitudinal space charge forces (LSC) and CSR. This is a fundamental instability with its roots in the shot noise in the electron distribution that provides an initial microbunching of electrons. After that the entire machine acts as an amplifier of this initial noise. What one gets at the end is an electron beam with a significant fragmentation in the longitudinal phase space and rather chaotic energy and spatial modulations. In analogy to

Landau damping, the "laser heater" was proposed [8,9] to weaken the instability by increasing the uncorrelated rms energy spread $\sigma_E$ thereby facilitating mixing of the microstructure developed in the electron beam.

Simulations of the microbunching instability with particle tracking codes require an unrealistically large number of macro-particles because of a numerical noise, unless suitable filters are used. In order to overcome this problem a new technique has been developed [10] that uses Vlasov's equation to follow the evolution of the 2D electron distribution function in the longitudinal phase space. The effect of transverse motion is accounted for by using a model of emittance-dependent mixing in the bunch compressors.

This technique is free from the numerical fluctuations suffered by macroparticle methods but care has to be taken to choose a sufficiently fine mesh where distribution function is defined to obtain adequate accuracy. Figure 3 shows 30 μm long segments of the electron distribution function at the end of BC2 calculated with this technique for the MB case using the laser heater producing $\sigma_E$ =10 keV and $\sigma_E$ =15 keV. Predictably, a larger energy spread leads to a weaker instability.

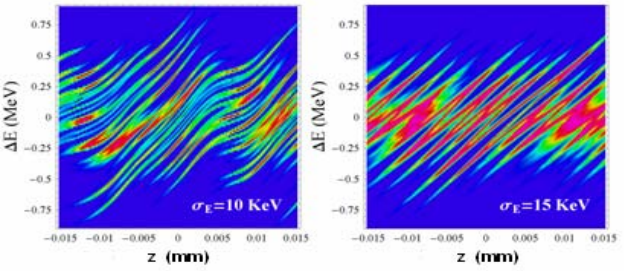


Figure 3. Fragments of the longitudinal phase space after BC2 for calculations with $\sigma_E$ =10 keV (a) and $\sigma_E$ =15 keV (b)

Figure 4 shows the rms slice energy spread at the end of BC2 as a function of energy spread introduced by the laser heater. Three different seeds generating the initial shot noise were used (except for the point at 11 keV where two seeds were used). The error bars span the range of the results.

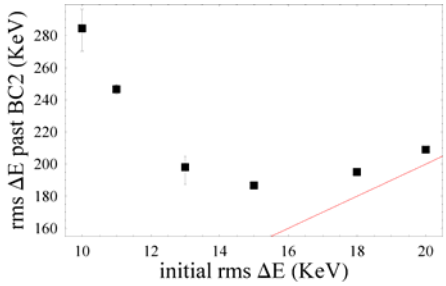


Figure 4. Uncorrelated slice energy spread as a function of the energy spread added by the laser heater calculated for MB case. Solid line shows the expected energy spread in the absence of any collective effects assuming compression factor of 10.

## SIMULATION RESULTS

Detailed simulations using *Elegant* [3] with 2 million macroparticles were performed for the MB and LB cases. They did not, however, include LSC effects because of the above mentioned problem of numerical noise. Figure 5 shows the longitudinal phase space and a histogram of the peak current for MB case and Figure 6 shows the same plots for the LB case.

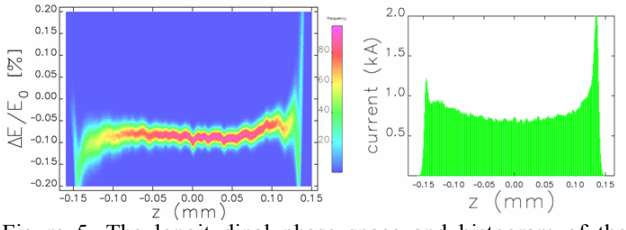


Figure 5. The longitudinal phase space and histogram of the peak current for the MB case. Initial energy spread $\sigma_E$ =15 keV.

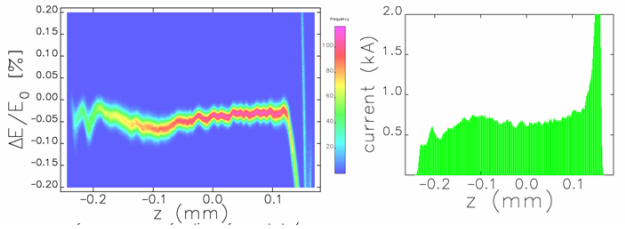


Figure 6. The longitudinal phase space and histogram of the peak current for the LB case. Initial energy spread $\sigma_E$ =20 keV.

Small-scale variations in both figures are likely caused by the instability. We intend to verify this assumption using IMPACT [11] with the inclusion of LSC effects and using 100 millions macroparticles. A distinct feature of the current results is that on the large scale they show a reasonably flat distribution in the longitudinal phase space (*i.e.* flatness of 3.6 MeV/ps$^2$ in the MB case and 1 MeV/ps$^2$ in the LB case) and flat histograms for the peak current. This is achieved by producing a linearly ramped peak current distribution in the injector. It has been shown in [12], by using a reverse tracking technique, that this distribution provides the above mentioned flat-flat output in the case of strong longitudinal wake fields acting along the accelerator.

Jitters in the phase and amplitude of the accelerating fields, electron bunch charge, and emission timing affect the electron beam. We have studied the sensitivity of the electron beam average energy, peak current and arrival time at the end of the accelerator to the various jitters and created a tolerance budget listed in Table 2 for MB case [13].

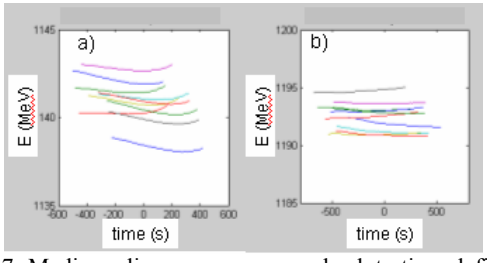


Figure 7. Medium slice energy versus absolute time defined by the master clock: a) MB case, b) LB case.

Jitters also affect the flatness of the electron bunches as can be seen form Figure 7, where median slice energy is

plotted against the absolute time defined by the master clock for the MB and LB cases, with ten randomly chosen seeds. The rms value of the flatness calculated over 400 seeds is ~1 MeV/ps$^2$ for MB case and ~0.5 MeV/ps$^2$ for LB case.

Table 2. Tolerance budget showing allowable rms jitters when the combined effect of all errors create an error in electron beam energy, peak current and arrival time with the rms value specified in the table. Parameters refer to accelerator section shown in Fig.1. The tighter tolerance is in bold text and all criteria are satisfied if the tighter tolerance is applied.

| Parameters | | Unit | $\lvert\Delta E/E_0\rvert$ <0.1% | $\lvert\Delta I/I_0\rvert$ <10% | $\lvert\Delta t_f\rvert$ <150fsec |
|---|---|---|---|---|---|
| L1 | $\varphi_0$ | deg | **0.10** | 0.20 | **0.10** |
| LX | $\varphi_1$ | deg | **0.30** | 0.50 | 0.70 |
| L2 | $\varphi_2$ | deg | **0.10** | 0.50 | 0.40 |
| L3 | $\varphi_3$ | deg | **0.10** | 0.20 | 0.20 |
| L4 | $\varphi_4$ | deg | **0.10** | 0.70 | 1.00 |
| L1 | $\Delta V_0/V_0$ | % | **0.10** | 1.00 | 0.15 |
| LX | $\Delta V_1/V_1$ | % | **0.50** | 0.80 | **0.50** |
| L2 | $\Delta V_2/V_2$ | % | **0.10** | 0.80 | 0.20 |
| L3 | $\Delta V_3/V_3$ | % | **0.10** | 0.50 | 0.15 |
| L4 | $\Delta V_4/V_4$ | % | **0.05** | 1.50 | 1.00 |
| Gun | $\Delta t_0$ | ps | **0.25** | 0.35 | 0.35 |
| | $\Delta Q/Q$ | % | **3.00** | 5.00 | 4.00 |

## BEAM BREAK-UP INSTABILITY

Due to the strong transverse wake potential in Linac 3 and Linac 4 [14], the beam break-up instability (BBU) appears to be the main source of projected emittance growth. Wake fields produced by leading electrons tend to bend the electron bunch in a characteristic "banana" shape. The origin of the instability is misalignment of accelerator elements including rf sections. Typical mis-alignment errors used in simulations are given in Table 3.

Table 3 Misalignment errors (rms values).

| | $\Delta x$, $\Delta y$ [μm] | $\Delta z$ [μm] | $\Delta\theta$ [μrad] |
|---|---|---|---|
| Dipole | - | - | 300 |
| Quadrupole | 150 | 200 | 300 |
| BPM | 150 | 200 | - |
| Acc. structure | 300 | - | - |

A convenient measure of the strength of the effect is the offset of the bunch tail with respect to the bunch head normalized by the beam transverse size $R = \Delta x / \sigma_x$. A histogram of $R$ obtained in a simulation of 120 trajectories with randomly chosen misalignment errors is shown in Fig.8. Although the effect is strong, it can be corrected by exploring the same wake fields that induce it in the first place. This may be achieved by beam steering and observing banana using slice emittance monitor. Figure 9 demonstrates the effect of the local trajectory bump in the area outlined with a dotted line. The change of the trajectory from a) to b) produced a reduction of $R$ from $|R| \approx 6$ to $|R| \le 1$.

Even when BBU, caused by misalignment, is compensated, some BBU will always exist and will jitter on pulse-to-pulse basis depending upon various jitters in the injector and power supply ripples in the accelerator. Fortunately, calculations show that this effect is rather small, typically producing $|R| \le 0.4$.

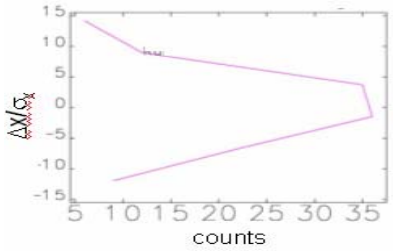


Figure 8. A histogram demonstrating the strength of the BBU (see explanation in the text)

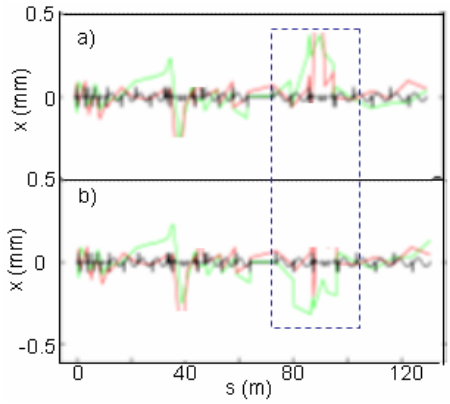


Figure 9. A change of the trajectory form (a) to (b) produced six fold reduction in the off-set of the electron bunch tail.

**Acknowledgement.** We are grateful to C. Bocchetta, J. Corlett and R. Ryne for many useful discussions.

## REFERENCES

[1] C. Bocchetta *et al.*, this conference
[2] S. Di Mitri *et al.*, Proc. of the FEL 2005 Conf., Stanford, USA (2005).
[3] M. Borland, APS LS-207, (2000).
[4] M. Borland *et al.,* NIM A. Res. A **483**, (2002)268.
[5] E.L. Saldin, E.A. Schneidmiller, and M.V. Yurkov, NIM A **490**, (2002)1.
[6] S. Heifets, G. Stupakov, and S. Krinsky, Phys. Rev. ST Accel. Beams **5**, 064401 (2002).
[7] Z. Huang and K.-J. Kim, Phys. Rev. ST Accel. Beams **5**, 074401 (2002).
[8] E.L. Saldin, E.A. Schneidmiller, and M.V. Yurkov, NIM A **528**, (2004)355.
[9] Z. Huang *et al.* PRST AB **7**, 074401 (2004).
[10] J. Qiang *et al*., J.Comp. Phys. **163**, (2000)434
[11] M. Venturini *et al*., LBNL Report, Berkeley LBNL-60513, (2006).
[12] M. Cornacchia *et al.*, this conference.
[13] P. Craievich, S. Di Mitri, this conference.
[14] P. Craievich, T. Weiland and I. Zagorodnov, NIM A **558** (2006)58